# Size-dependent transition from shape to exchange dominated magnetic nanostructure

W. Casey Uhlig[a] and John Unguris
*Electron Physics Group, National Institute of Standards and Technology, Gaithersburg, Maryland 20899*

(Presented on 1 November 2005; published online 18 April 2006)

In order to quantitatively investigate the interplay between shape anisotropy (magnetostatics) and exchange, patterned zigzag structures were prepared with sizes varying over two orders of magnitude. The magnetic state is a balance between shape anisotropy, which causes the magnetization to follow the serrated edge of the structure, and exchange, which prefers uniform magnetization. In intermediate-sized structures, we find that the magnetization along the center of the zigzag oscillates between approximately ±32° and is relatively independent of the device size. As the dimensions are reduced to less than a critical length $\lambda_{cr}$, the oscillation magnitude drops rapidly. On the other hand, the largest structures develop extended film properties such as multiple vortices and ripple. © *2006 American Institute of Physics*. [DOI: 10.1063/1.2163274]

Magnetization states and reversal modes of mesoscopic magnetic elements can be strongly controlled by shape.[1–8] Controlling these properties is essential for magnetoelectronic device performance. However, as the scale of device dimensions shrinks, the exchange stiffness becomes more influential on the domain configurations; thus, device control by shape becomes less effective. On the other hand, very large structures are more immune to the effects of shape as magnetostatic energies associated with edge structure become less significant. Though these basic concepts are generally expected, quantitative studies are few. Here, we systematically study the evolution of magnetic structure through these three regions of interest: extended film (very large structures), shape dominated (intermediate structures), and exchange dominated (very small structures).

The zigzag[9] configuration (see Fig. 1) is chosen because the magnetization state can be strongly correlated to the serrated edge of the structure. This results in the biasing of the magnetization alternately away from the long axis of the structure in a regular and reproducible manner. Thus, this shape lends itself to a comprehensive study of the interplay between the exchange stiffness and shape anisotropy. To investigate the three regions of interest, the size of the patterned zigzag structures is varied over more than two orders of magnitude.

The structures were fabricated using electron beam lithography and lift-off of a 12 nm thick NiFe film with cell dimensions ranging from $100\times200$ nm to $20\times40$ $\mu$m. (All structures used cells of aspect ratio 2.) We used scanning electron microscopy with polarization analysis (SEMPA) to image the magnetization because it is uniquely able to quantitatively measure the magnetization over this large size range while maintaining constant resolution (≈10 nm) and contrast. The extent of the dimensional range is illustrated in Fig. 1, which shows SEMPA images ranging from the largest to smallest cell sizes. To highlight the wide size range, the image of the smallest device is also shown inside the blue circle on the same scale as the largest device. The magnetization direction is represented by color as indicated by the color wheel shown in the figure. All SEMPA images throughout the paper are of the virgin magnetic state and are presented using the same color wheel scheme.

A key characteristic of the zigzag pattern is the distance from peak to valley along the length of the structure or minimum feature size, $\lambda_m$, as indicated in Fig. 1. This is the length scale in which the magnetization must be able to respond to conform to the structural shape. Therefore, further scaling presented in this work will be in reference to $\lambda_m$.

Several distinguishing characteristics can be seen for the two largest structures in Fig. 1. These possess qualities of the extended film regime. The presence of multiple vortices, ripple, and the nonideal conformity of the magnetization to the shape leads to nonreproducible remanent states. For instance, the magnetization angle in the $\lambda_m=14$ $\mu$m structure does not oscillate uniformly, in magnitude or periodicity, away from the long axis. Though the average deflection amplitude is 39°, several degrees larger than zigzags from the intermediate region, the standard deviation is ±6°, in contrast to the uniform response of smaller structures (order of ±1°).

A measure of how well the magnetic structure follows the physical structure is given by a line scan along the center of the structure as shown in Fig. 2. The amplitude of the oscillation, $A$, is determined by fitting the line-scan data to a sinusoidal curve. The magnetic structure in the intermediate-sized patterns is dominated by magnetostatics from the edges. Thus, structures in this region most ideally conform to shape, i.e., the shape dominated regime. Figure 2 shows the domain state of a $1\times2$ $\mu$m cell or $\lambda_m=0.7$ $\mu$m structure with an arrow map overlay. The single vortices present in the ends of the structure are common features on this size scale, separated by uniform deflections away from the long axis through the device. A sinusoidal fit to the line scan yields $A=31°\pm1°$. This is very typical of the structures with $\lambda_m$ from approximately 5 $\mu$m down to 300 nm, where $A$ is relatively constant with an average of 32°. (Across the short axis of the zigzags at the oscillation peak, the magnetization re-

[a]Electronic mail: willard.uhlig@nist.gov

 

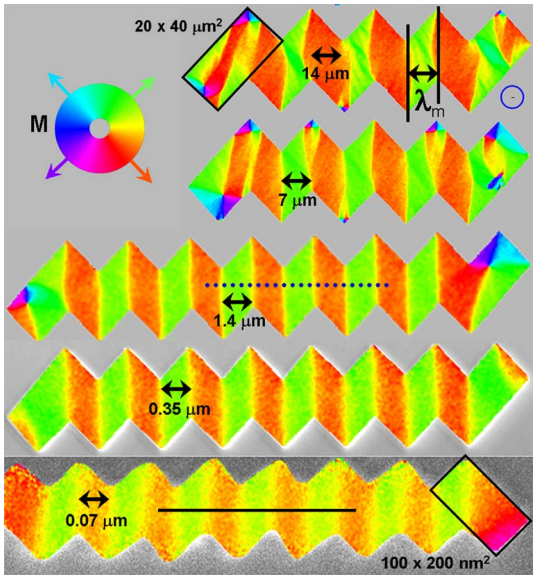


FIG. 1. (Color online) SEMPA images of 12 nm thick NiFe zigzag structures. The cell size was varied from $20\times40$ $\mu$m down to $100\times200$ nm. The speck inside the blue circle at the upper right of the figure is a copy of the bottom image to scale with the top structure. $\lambda_m$ is the minimum feature size. The blue dotted and solid black lines along the 1.4 and 0.07 $\mu$m $\lambda_m$ devices illustrate where line scans, which are shown in Fig. 3, were extracted from the image. The color wheel denotes the direction of the magnetization.

laxes from about 45° at the top and bottom edges of the structure down to 32° along the center line.[9])

As $\lambda_m$ is reduced to nanoscale dimensions, the magnetization response to the serrated edge drops rapidly. The image of the 0.07 $\mu$m $\lambda_m$ device in Fig. 1 almost seems faded or washed out. This apparent lack of contrast is solely due to the fact that the magnetization is becoming more uniform along the long axis (yellow on the color wheel). The blue dotted and solid black lines represent where line scans were extracted from the image data. These line scans are compared in Fig. 3. The $x$ axis on the line-scan data has been normalized to the periodicity of the structures ($2\lambda_m$), and shows a significant drop in following the serrated edge; $A$ drops from 32° to only 15°.

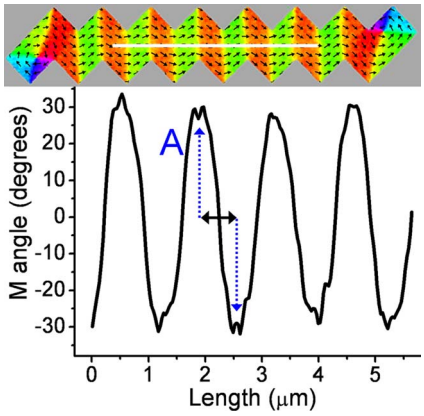


FIG. 2. (Color online) The SEMPA image and line scan of a $1\times2$ $\mu$m cell ($\lambda_m$=0.7 $\mu$m) structure. An arrow map overlay of the image shows the magnetization direction, while the white solid line indicates where the line-scan data were acquired. The average oscillation amplitude, $A$, of the magnetization direction is defined as the amplitude of a sinusoidal fit to the data.

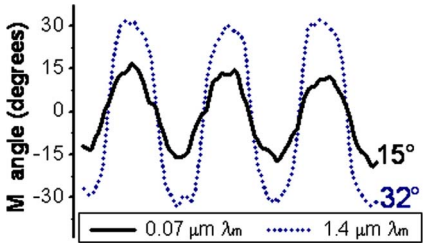


FIG. 3. (Color online) Line scans from SEMPA images along the long axis of 0.07 and 1.4 $\mu$m $\lambda_m$ structures, showing how the ability of the magnetization to follow the structure edge is diminished as device dimensions are decreased.

This abrupt transition in magnetization behavior with device size is shown quantitatively in Fig. 4. Hollow circles represent the SEMPA line-scan measurements of $A$ as fit by the sinusoidal curve. Linear fits were performed in two regions, for data above a minimum feature size of 300 nm and data below 200 nm. Though the data above $\lambda_m$ of 1.5 $\mu$m are cut off from the plot, they were included in the linear fit. We define the critical length $\lambda_{cr}$ as the intersection of the two fits. The transition point occurs at $170\pm10$ nm. Structures with $\lambda_m<\lambda_{cr}$ are strongly dominated by the exchange interaction.

To better understand how this transition point relates to length scales defined by the exchange energy and magnetostatics, we compare $\lambda_{cr}$ with the typical domain wall width, which can be calculated as

$$\lambda_{dw}=\pi\sqrt{A_{ex}/K}.$$

$A_{ex}$ is the exchange stiffness ($1.3\times10^{-13}$ J/m for NiFe) and $K$ is the anisotropy of the element. It has been shown previously[10] that for a thin narrow stripe of width $w$ and thickness $d$, magnetization reversal can be appropriately predicted by modeling the anisotropy as

$$K\approx\frac{3M_s^2d}{2w},$$

where $M_s$ is the saturation magnetization. Therefore, $\lambda_{dw}$ varies as the square root of $w$. Although $\lambda_{dw}$ describes a 180° domain wall, we use this as an upper bound. If $\lambda_{dw}$ ($\propto\sqrt{w}$) is larger than $\lambda_m$ ($\propto w$), the magnetization can no longer effectively respond to the edge structure. Using the cell width of

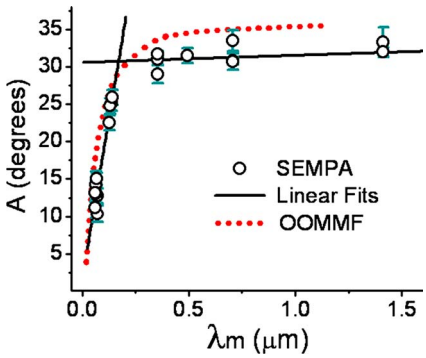


FIG. 4. (Color online) A summary of the magnetization oscillation amplitude as a function of the minimum feature size. The solid lines represent linear fits to the data with $\lambda_m$ above 300 nm and below 200 nm. The dotted line represents micromagnetic simulations using an ideal zigzag structure.

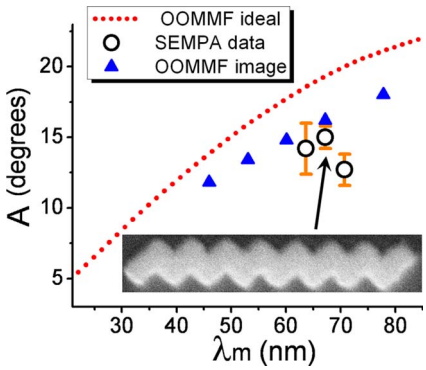


FIG. 5. (Color online) A closer look at the data from the smallest zigzag structures. Results from OOMMF simulations, using the inset SEM image (corresponding to the center data point) as a mask, are represented by the triangles.

the zigzag structure as $w$, this narrow stripe approximation gives an intersection of $\lambda_m$ and $\lambda_{dw}$ of 220 nm. Thus, the length scale of the observed crossover is very reasonable.

The rapid decrease in oscillation amplitude has also been observed in micromagnetic simulations.[11] OOMMF simulations[12] were performed on ideal zigzag structures varying $\lambda_m$ from 1.1 $\mu$m to 18 nm. These data are represented by the dotted line of Fig. 4. Applying linear fits to the more linear regions of the OOMMF curve (below 100 nm and above 300 nm), yields a transition point of $152 \pm 12$ nm. As can be seen, the simulations consistently yield larger off-axis angles than the actual data.

In the smaller structures, where the shape becomes somewhat more rounded and less ideal, the use of the actual SEM images as masks improves the agreement of the simulations, as shown in Fig. 5. The micrograph inset in Fig. 5 is the smallest device in Figs. 1 and 3. The triangles indicate simulations using this image as a mask and varying the size. The dotted line again represents OOMMF simulations using an ideal zigzag shape. Thus, the quality and sharpness of the shape can also strongly affect the magnetization. Though this result is somewhat obvious, it underscores the importance of using a realistic shape in micromagnetic simulations. Nevertheless, the measured change in magnetization with size (Fig. 4) appears to be much greater than any loss incurred from the quality of shape as the structure size was reduced.

In conclusion, by utilizing the unique capabilities of SEMPA, we have observed three distinct regions of behavior in NiFe patterned zigzags: extended film, shape dominated, and exchange dominated. Structures having minimum feature sizes on the order of several microns and larger display many common extended film properties and cannot be consistently controlled by shape. The region consisting of structures with $\lambda_m$ from approximately 5 $\mu$m down to a critical length $\lambda_{cr}$, on the order of 200 nm, can be controlled reliably by shape and exhibit reproducible magnetic responses for device applications. Below $\lambda_{cr}$, the magnetization state begins to be dominated by the exchange energy. In this region, the ability to manipulate devices by shape begins to rapidly diminish.

This work has been supported in part by the Office of Naval Research.

[1] R. M. H. New, R. F. W. Pease, and R. L. White, J. Vac. Sci. Technol. B **13**, 1089 (1995).
[2] S. Y. Chou, P. R. Krauss, and L. Kong, J. Appl. Phys. **79**, 6101 (1996).
[3] K. J. Kirk, J. N. Chapman, and C. D. W. Wilkinson, Appl. Phys. Lett. **71**, 539 (1997).
[4] Y. Chen, V. Kottler, F. Carcenac, J. F. Rene, N. Essaidi, C. Chappert, and H. Launois, J. Vac. Sci. Technol. B **16**, 3830 (1998).
[5] M. Hermann, S. McVitie, and J. N. Chapman, J. Appl. Phys. **87**, 2994 (2000).
[6] W. Y. Lee, C. C. Yao, A. Hirohata, Y. B. Xu, H. T. Leung, S. M. Gardiner, S. McPhail, B. C. Choi, D. G. Hasko, and J. A. C. Bland, J. Appl. Phys. **87**, 3032 (2000).
[7] J. Shi, S. Tehrani, and M. R. Scheinfein, Appl. Phys. Lett. **76**, 2588 (2000).
[8] W. C. Uhlig, H. Li, B. S. Han, and J. Shi, J. Appl. Phys. **91**, 6943 (2002).
[9] F. C. S. da Silva, W. C. Uhlig, A. B. Kos, S. Schima, J. Aumentado, J. Unguris, and D. P. Pappas, Appl. Phys. Lett. **85**, 6022 (2004).
[10] W. C. Uhlig and J. Shi, Appl. Phys. Lett. **84**, 759 (2004); J. Appl. Phys. **95**, 7031 (2004).
[11] M. J. Donahue and D. J. Porter, *OOMMF's User Guide*, Version 1.0, NISTIR 6376 (National Institute of Standards and Technology, Gaithersburg, MD, 1999). For more information, see the website at http://math.nist.gov/oommf/.
[12] M. J. Donahue, F. da Silva, and D. P. Pappas, Presentation at the Magnetism and Magnetic Materials Conference 2004, Jacksonville, FL, 8 November 2004.